



# Removal of artificial anionic dye by electrocoagulation and electro-oxidation combined system using aluminum and nano (Cu-Mn-Ni) composite electrodes

Reman A. Jasim <sup>a,\*</sup>, Rasha H. Salman <sup>a</sup>, Muhannad K. Zabar <sup>b</sup>

<sup>a</sup> Department of Chemical Engineering, College of Engineering, University of Baghdad, Aljadria, Baghdad, Postcode: 10071, Iraq

<sup>b</sup> Department of Chemical Engineering, Curtin University, Australia

## Abstract

The combined system of electrocoagulation (EC) and electro-oxidation (EO) is one of the most promising methods in dye removal. In this work, a solution of 200 mg/l of Congo red was used to examine the removal of anionic dye using an EC-EO system with three stainless steel electrodes as the auxiliary electrodes and an aluminum electrode as anode for the EC process, Cu-Mn-Ni Nanocomposite as anode for the EO process. This composite oxide was simultaneously synthesized by anodic and cathodic deposition of Cu (NO<sub>3</sub>)<sub>2</sub>, MnCl<sub>2</sub>, and Ni (NO<sub>3</sub>)<sub>2</sub> salts with 0.075 M as concentrations of each salt with a fixed molar ratio (1:1:1) at a constant current density of 25 mA/cm<sup>2</sup>. The characteristics structure and surface morphology of the deposited nano oxides onto the graphite substrates were determined by (XRD), (FE-SEM), (AFM), and (EDX). The results shown that nano Cu-Mn-Ni oxides were successfully deposited onto the anode and cathode. The crystal size and root mean square for the cathode were 30.79 nm and 79.36 nm, respectively, while for the anode, they were 24.19 nm and 41.88 nm, respectively. Furthermore, the combined system was examined for C.D, NaCl concentration, and time. In the EC-EO combined system, the cathode and anode were efficient when used as anodes for the EO process, besides aluminum. The cathode was more effective in the removal process than the anode due to its larger crystal size and the rough, granular shape of its surface. When current density (C.D) increased from 3 to 6 mA/cm<sup>2</sup>, the removal efficiency shifted from 95% to 98%. However, excellent removal of 98% and 96.5% was attained with 1.665 and 2.0859 kWh/kg of dye as energy consumption in the presence and absence of NaCl salt, respectively by applying 6 mA/cm<sup>2</sup> within 20 min of electrolysis.

*Keywords:* Electrodeposition; composite electrode; Electrocoagulation; electro-oxidation; combined system; Congo red.

*Received on 06/05/2024, Received in Revised Form on 07/07/2024, Accepted on 07/07/2024, Published on 30/12/2024*

<https://doi.org/10.31699/IJCPE.2024.4.4>

## 1- Introduction

Water is an essential element for human life and living organisms on Earth. However, the development of modern social lifestyles and the industrial revolution in the twentieth century had a major impact on the increase in pollutants released into the environment. Pollutants are a mixture of various types of toxic material thrown up daily in water resources, and they have different undesirable impacts on the environment depending on their properties [1].

Numerous contaminants are introduced to the environment from industrial processes, which are destroying the ecosystem and affecting human health and the economy. Wastewater containing dyes have received significant attention hence dyes are widely used in many industries, including textile, tanning, printing, and food. These industries consume a significant amount of water during the manufacturing process [2, 3].

Azo dyes are one of the most important manufacturing dyes used in different processes, they consist of aromatic components with two azo bonds N=N, and it is classified

as highly toxic materials because of the presence of the nitrogen group. Congo red is an azo dye used in various industries such as printing, dyeing, pH indicators, rubber industries, and especially in textile industries because of its strong convergence and low cost. However, it is a concerning pollutant as it can cause genetic mutations and cancer in humans, and harms aquatic ecosystems. Therefore, Congo red wastewater must be treated to reduce its concentration and ensure it meets acceptable levels before being discharged into rivers. Numerous methods for Congo red degradation were utilized such as biodegradation with aerobic and non-aerobic bacteria, adsorption, membrane filtration, photocatalytic, chemical coagulation, and electrochemical process [4, 5].

Electrochemical technology is a clean, environmentally friendly method that does not require the addition of many chemicals, it used for treating various types of contaminants and dyes and it generates chemical components in situ on the electrode surface by consuming low energy. Many electrotechnology used for eliminating Congo red in wastewater like electro-Fenton [6],



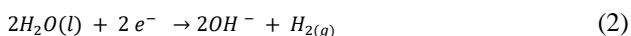
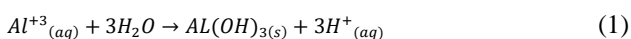
\*Corresponding Author: Email: [rayman.jassim2207m@coeng.uobaghdad.edu.iq](mailto:rayman.jassim2207m@coeng.uobaghdad.edu.iq)

© 2024 The Author(s). Published by College of Engineering, University of Baghdad.

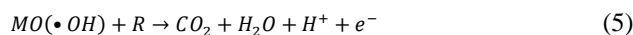
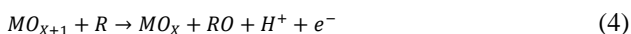
This is an Open Access article licensed under a [Creative Commons Attribution 4.0 International License](https://creativecommons.org/licenses/by/4.0/). This permits users to copy, redistribute, remix, transmit and adapt the work provided the original work and source is appropriately cited.

ozonation [7], direct and indirect electro-oxidation [8], and electrocoagulation [9].

One of the most efficient methods for Congo red degradation is electrocoagulation (EC), it is a simple operation, does not need chemical additives, produces less amount of sludge than chemical coagulation, it is easy to control, and operates with low consumed energy. It depends on several parameters such as electrode type, pH, dye concentration, and current density. Aluminum and iron are the most common electrode used in electrocoagulation [9]. The EC process involved the generalization of a coagulant component in situ by applying external power on the electrodes where metal ions ( $M^+$ ) are released from the dissolution of the sacrificial electrode. Water electrolysis generates hydrogen ions ( $H^+$ ) and hydroxyl ions ( $OH^-$ ), which react in bulk solution to generate metal hydroxide, destabilizing dye particles, adsorbing them, and aggregating them together. However, enlarged particles were precipitated due to gravitational force, and particles with small sizes floated with the help of gases bubbles of oxygen ( $O_2$ ) and hydrogen ( $H_2$ ) generated on the anode and cathode surfaces, respectively, the EC process mechanism can be shown in the following Eqs. 1-3 [10].



Another electrochemical process is electro-oxidation (EO), it is used to remove a wide range of organic pollutants and can oxidize the dyes and convert them to Carbon dioxide ( $CO_2$ ) and water. Electro-oxidation efficiency depends on the acidity, and alkalinity of a solution, the intensity of current density applied, electrode type, and salt addition as supporting electrolytes. EO can be classified as a direct and indirect process. The direct electro-oxidation process depends on the efficiency of the anode for generating hydroxyl radical ( $OH^*$ ) as an oxidizing agent, so it is called anodic oxidation. Two types of electrodes are used in direct electro-oxidation with different behaviors, active electrodes which cause chemisorbed species (oxygen present in  $MO_{x+1}$ ) which causes selective oxygen product as shown in Eq. 4, and non-active electrodes which cause physically adsorbed species (adsorbed hydroxyl radical  $OH^*$ ) which completely oxidized of the organic component to  $CO_2$  and  $H_2O$  as shown in Eq. 5. In indirect electro-oxidation, strong oxidized agents are added to the solution such as  $H_2O_2$ , and NaCl, etc. [8]. When NaCl is added to the electrolytic solution, an oxidizing agent like hypochlorous acid ( $HOCl$ ) and hypochlorite ion ( $OCl^-$ ) would be produced based on pH value. In acidic conditions,  $HOCl$  would be produced which is more efficient than ( $OCl^-$ ) [11].



Different types of electrodes are utilized for the electro-oxidation process such as Boron-Doped electrodes (BBD), multi-metal oxide electrodes (MMO), stainless steel, and graphite. To overcome prevalent electrode problems such as low stability and corrosion, it is necessary to synthesize a new type of electrode with high efficiency by coating the surface of the substrate with nano oxide to give them the desired specification [12, 13]. One of the methods used for composite electrode preparation is the electrodeposition technique which is used to modify substrate properties by coating its surface with a thin film of metal oxide, nano metal oxide has several advantages such as low cost, high stability, high surface area, and low operation temperature which make the substrate more efficient.  $Cu_2O_3$ , NiO, MnO, and  $Fe_2O$  are examples of metal oxides that can be deposited as binary or ternary on the surface of the substrate. A few studies succeeded in depositing metal oxide on the cathode and anode simultaneously [14, 15].

Sometimes two or more electrochemical removal methods are combined to overcome problems found with a single method. The hybrid removal process (EC-EO) is used to enhance the degradation efficiency and reduce time and power, no previous studies have used a combined process (EC-EO) for Congo red dye removal.

The goal of the present work is to investigate the efficiency of a hybrid combined system (EC-EO) to remove Congo red dye by using Al substrate as a sacrificial anode for the EC process, and composite electrode (cathode or anode) which is produced by electrodeposition of nano metal oxide (Cu-Mn-Ni) as anode for the EO process. Besides, studying the effect of three parameters (current density (C.D), NaCl concentration, and electrolysis time) on this combined system.

## 2- Experimental works

### 2.1. Chemicals

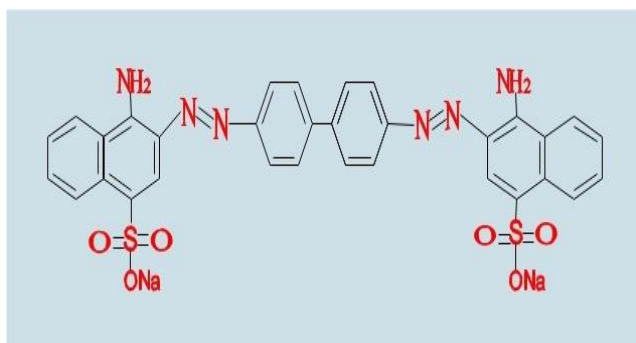
Distilled water was used in the preparation of aqueous solutions, and all chemicals were of high purity and there was no need for further purification. The utilized chemicals were:  $Ni(NO_3)_2 \cdot 6H_2O$  (with a purity of 99.0%, Central Drug Hense),  $MnCl_2 \cdot 4H_2O$  (with a purity of 98.0%, Techno Pharmchem)  $Cu(NO_3)_2 \cdot 3H_2O$  (with purity 99%, HIMEDIA), HCl (37%, liquid, Sigma-Aldrich), Congo red (with a purity of 99.0%, ANJDULY), NaCl (with a purity of 99.5%, Avonchem), and  $Na_2SO_4$  (with purity of 99%, LOBA CHEMIE).

### 2.2. Congo red dye properties

The properties of Congo red are illustrated in Table 1 [16], and Fig. 1 shows the molecular formula of the dye.

**Table 1.** Congo red properties

Congo red dye	Properties
Molecular weight	696.68 g/mol
Density	4.25 g/cm <sup>3</sup>
Melting point	>360 °C
Chemical formula	C <sub>32</sub> H <sub>22</sub> N <sub>6</sub> Na <sub>2</sub> O <sub>6</sub> S <sub>2</sub>
Chemical/Dye Class	Azo dye
No. of Azo dyes color	2 bonds
Color index	Blue<3, Red>3
Maximum wavelength	2000-229999
Behavior in water	488 μm- 497μm
	Very slightly soluble in acetone, practically insoluble in xylene and ether, and soluble in water.

**Fig. 1.** Congo red dye structure

### 2.3. Experimental work

#### 2.3.1. Preparation of Cu-Mn-Ni nano metal oxide electrode

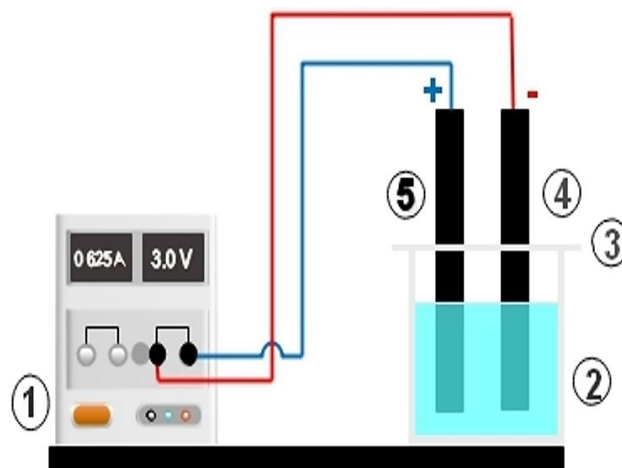
Deposited Cu-Mn-Ni nano metal oxide on the surface of graphite substrate was classified into two steps, the first step is the pretreatment of graphite substrate before the electrodeposition process and it includes the removal of any oxide layers and impurities by activating the graphite substrates with 350 °C by (N20/H W-Germany) furnace for 30 minutes, then smoothen it by using 320-grit sandpaper and submerged it with acetone to obtain a surface with high purity and finally washed it with distilled water.

In the second step, a batch electrolytic cell was used to simultaneously deposit of Cu-Mn-Ni nano metal oxide on the cathode and anode of a graphite substrate measuring 15cm×15cm×3mm. The graphite substrate was submerged vertically inside a beaker, with only a 5x5 cm area of graphite substrate immersed in the electrolyte. There was a 3 cm distance between the two electrodes and a 1cm distance from the bottom of the beaker, as illustrated in Fig. 2. The electrolytic solution was prepared by dissolving 0.075 M of each metal salt Cu(NO<sub>3</sub>)<sub>3</sub>H<sub>2</sub>O, MnCl<sub>2</sub>·4H<sub>2</sub>O, and Ni(NO<sub>3</sub>)<sub>2</sub>·6H<sub>2</sub>O in 0.35 L of distilled water with 1:1:1 as mixing molar ratio, for 3 h (1.5 h for each substrate side). A fixed current density was applied with a 25 mA/cm<sup>2</sup> value at room temperature 27°C ± 2, and no agitation was used.

The composite electrodes (cathode and anode) were washed with distilled water and left to dry in the air, and to obtain a more stable Cu-Mn-Ni nano metal oxide layer on the surface of the substrate, the electrodes were

calcination at 400 °C in (N20/H W-Germany) furnace, for one hour was accomplished.

The characteristics of the Cu-Mn-Ni composite electrode surface were examined by X-ray diffraction (XRD), energy dispersive X-ray (EDX), field scanning electron microscope (FESEM), and atomic force microscopy (AFM). Composite electrodes (cathode and anode) were used as an anode for the electro-oxidation process besides Al as an anode for electrocoagulation in the combined EC-EO system to remove Congo red dyes.

**Fig. 2.** Electrodeposition cell setup, 1. DC power supply, 2. Electrolyte cell, 3. Perspex cover, 4. Graphite cathode, 5. Graphite anode

#### 2.3.2. Congo red removal by EC-EO combined system

EC-EO combined system was utilized to remove congo red in a batch reactor made from Perspex. The utilized electrodes were three stainless steel plates (type 316) with 3mm thick which were the auxiliary electrodes and an Al plate with 4mm thick fixed between two stainless steel electrodes as anode for the EC process. The anode for the EO process was the prepared composite (either cathode or anode) with 3mm thick which was fixed between two stainless steel cathodes as shown in Fig. 3. A 2cm gap between each two electrodes was kept, and a Perspex cover with five holes was used and two holes existed for the thermometer and pH probe (OHAUS Corporation, USA). A monopolar connection was utilized for all electrodes and a power supply (MAISHENG MS-605D) was used to supply the required current to the electrodes. each electrode had a fixed dimension of length and width (15cm×15cm) and the effective surface area of each side of the Al anode and Cu-Mn-Ni composite was 25 cm<sup>2</sup> which means that the total active area of two anodes was 100 cm<sup>2</sup>, and the system's temperature was kept at about 27°C ± 2.

A simulated Congo red solution was prepared by dissolving 200 mg/l of Congo red dye, the quantity of treated solution was 2 L of distilled water, therefore 400 mg of Congo red was dissolved to attain the required concentration. A 0.02 M of Na<sub>2</sub>SO<sub>4</sub> salt was added in all experiments to increase the conductivity of the electrolyte

without affecting removal efficiency, 0.1M of HCl was added before the electrolysis process to justify the pH at 7, and the solution was mixed at 250 rpm by using (Heidol pH™ 505-20000-00, 0-300 °C; 0-1400 rpm) magnetic stirrer to ensure a homogeneous mixture.

Several parameters were investigated to conclude their effect on the efficiency of the combined system for dye removal, current density between 3 and 6 mA/cm<sup>2</sup>, 0 to 0.5 g/l of NaCl conc., 10 ml of samples were drawn every 5 min within 20 min of electrolysis, the sample was left to precipitate for 1h, and then by using UV-Vis-9200 (BIOTECH ENGINEERING MANAGEMENT CO.LTD. (UK), the light absorbency of Congo red dye determined at λ<sub>max</sub> =494nm., and Eq. 6 determines the efficiency of dyes degradation [17].

$$\% \text{ Congo red dye removal} = \frac{(C_i - C_f)}{C_i} \times 100 \quad (6)$$

Where C<sub>i</sub> represents the initial concentration before treatment and C<sub>f</sub> represents the final concentration after treatment in mg/l.

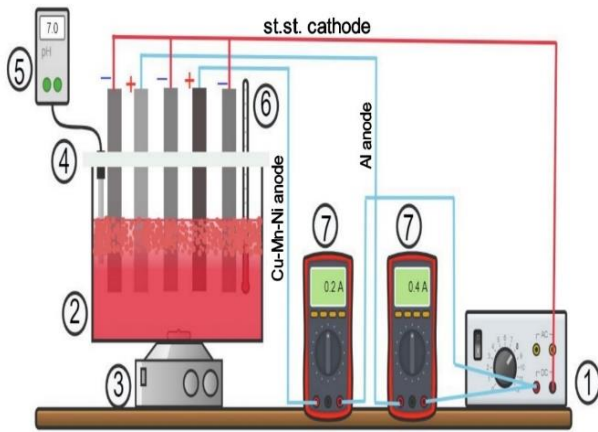


**Fig. 3.** A schematic diagram of the combined cell: 1. DC power supply, 2. Perspex cell, 3. Magnetic stirrer, 4. Perspex cover, 5. pH meter, 6. Thermometer, 7. Multimeter

### 3- Results and discussion

#### 3.1. XRD analysis

Fig. 4 represents the crystal structure of Cu-Mn-Ni nano metal oxide on the cathode (C) and anode surface (A), by XRD (X-ray powder diffractometer) analytical X' Pert Pr UK. Diffraction data was obtained for 2θ by using Cu-Kα radiation (λ=1.5406 Å), with voltage 40kv, and current of 30 mA from 10° to 80°. It was employed to detect crystal phase and size, it proved the appearance of several metal oxides on the surface of graphite substrates (cathode and anode) such as CuO with cubic and Monoclinic phase, at 26.67°, 35.91°, 54.86°, and 77.54° peaks corresponding to hkl -111,111,020, and 222, respectively, and that agree with standard pattern JCPD card no. 001-1117 and JCPD card no. 078-0428.

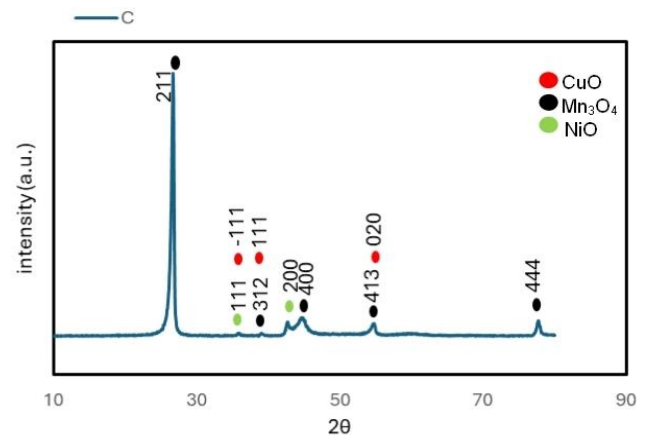
Another oxide that presented was the Mn<sub>3</sub>O<sub>4</sub> with Tetragonal phase at 2θ of 26.76°, 39.05°, 54.75°, and 77.69° which was corresponded to hkl of 211,312,400,413, and 444 respectively that coincided well with pattern JCPD card no.-075-1560.

The cubical structure of NiO was also detected on the graphite surface which agrees with the pattern JCPD card no. 00-047-1049 with peaks at 2θ of 35.91°, and 42.69° which match with hkl 111 and 200, respectively. A strong peak at the 2θ value was shown at about 26.6° for graphite [18].

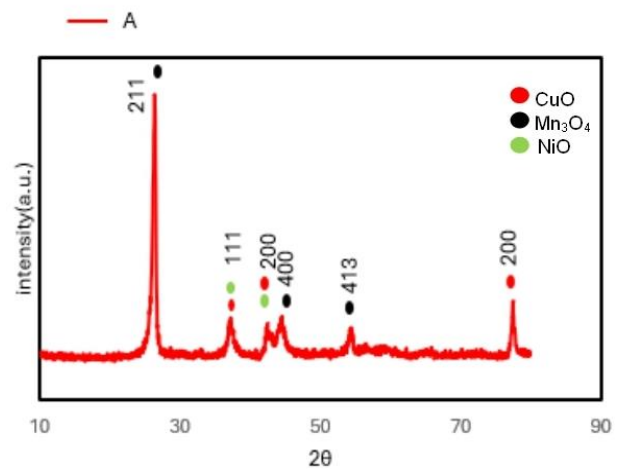
The cathode has more crystallinity than the anode, the average crystal size of the cathode was 30.79 nm and of the anode 24.19 nm and it was obtained by applying the Scherrer equation as shown in Eq. 7.

$$\text{crystal size} = \frac{k\lambda}{\beta \cos\theta} \quad (7)$$

where K is the factor of dimensional shape about 0.9, λ is the X-ray wavelength which is equal to 1.5404 Å, θ is Bragg angle and β is the line broadening at half the maximum intensity (FWHM) [19].



(a)



(b)

**Fig. 4.** XRD for Cu-Mn-Ni nano metal oxide deposit at 0.075 M concentration with fixed molar ratio 1:1:1, Current Density = 25mA/cm<sup>2</sup>, Time 3h, (a) on the Cathode, (b) on the Anode

### 3.2. FE-SEM analysis

The performance of any electrode can be concluded from its morphology structure. The morphology of CuO, Mn<sub>3</sub>O<sub>4</sub>, and NiO nano metal oxide which were deposited on the surface of the C cathode and A anode was examined by FE-SEM analysis (field emission scanning electron microscopy-imaging-EDS-Mapping-Line EBSD-

Germany with the 25 KV). Small spherical crystals resulted randomly on the surface of the cathode (C) and it was accumulated together, while at the anode (A), they appeared like bubbles spread on the surface. At the cathode, the growth rate was increased while at the anode, the nucleation rate was increased as seen in Fig. 5, a picture taken with two magnifications of 10 kx and 50 kx, this result agreed with the previous study [20, 21].

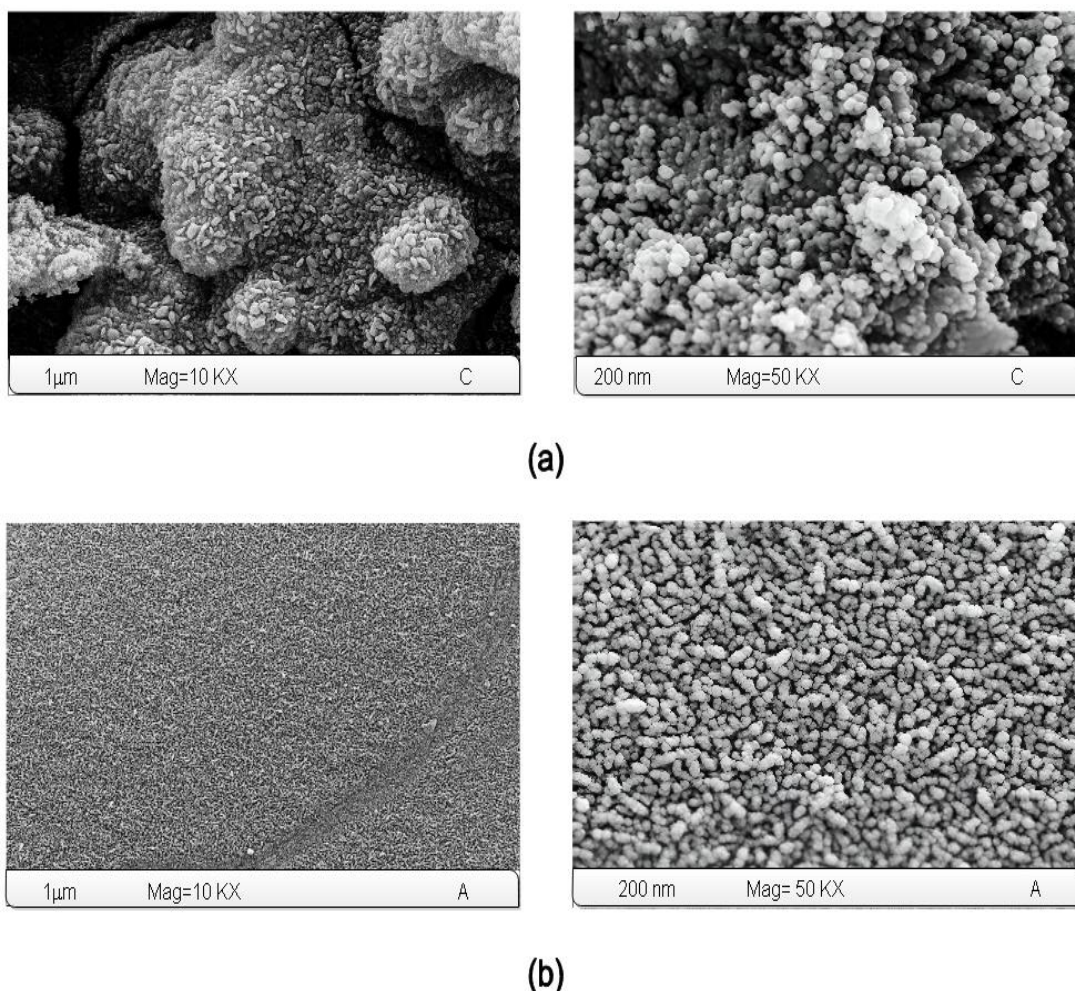


**Fig. 5.** FE-SEM image of Cu-Mn-Ni nano metal oxide at different magnifications (10kx-50kx) For (a) Cathode, (b) Anode, prepared at fixed molar ratio (1:1:1), at 25mA/cm<sup>2</sup>, and Time 3h

### 3.3. EDX analysis

To detect the chemical composition of each deposited component, EDX analysis (energy dispersive X-ray) was applied, which proved that metal oxide formed on the surface of the cathode and anode. O, Cu, Mn, and Ni elements appeared on the surface of the C cathode and A anode. Fig. 6 determines the weight percentage for each element on the cathode and anode. It is known that the amount of substance deposited is affected by many parameters like temperature, the concentration of metal salt, the dissolving of metal with solution, and its ability for reduction and oxidation reaction [22, 23]. Therefore, the results of Fig. 6 illustrated that Mn was mainly deposited with the highest wt. percentage onto anode while Cu had the highest wt. percentage onto the cathode.

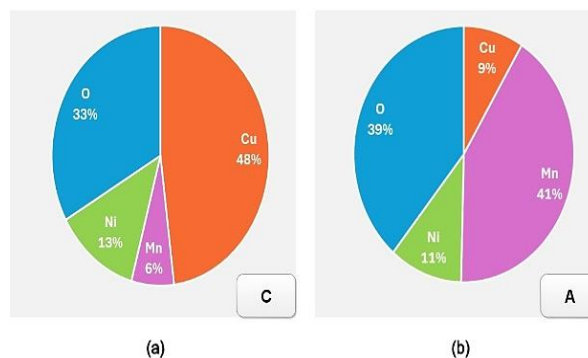


**Fig. 6.** EDX of Cu, Mn, and Ni oxides at fixed mixing molar ratios 1:1:1, (a) Cathode, (b) Anode

### 3.4. AFM analysis

The AFM technique is used to recognize the roughness, and average mean diameter of layers grown on the surfaces, a thin film of Cu-Mn-Ni nano metal oxide was detected on the surface of graphite (C cathode and A anode). From Fig. 7, a histogram of particle size and the distribution of accumulated grains are shown. The particle size for the cathode and anode was 30.79 nm, and 24.19 nm, respectively. Hydrogen evolution on the C cathode causes a deposit of nano metal oxide with a larger size and roughness on its surface than the A anode, which is

consistent with the previous study [14]. The root mean square and roughness for the cathode and anode are shown in Table 2. The resulting nano size for prepared electrodes gave them significant properties such as large surface area and more active sites for reaction [24].

**Table 2.** The root-mean-square height, and roughness for Cu-Mn-Ni Cathode (C) and Anode (A)

Electrodes	root-mean-square, nm		roughness, nm	
	Cathode	Anode	Cathode	Anode
Cu-Mn-Ni	79.36	41.88	1.987	0.9

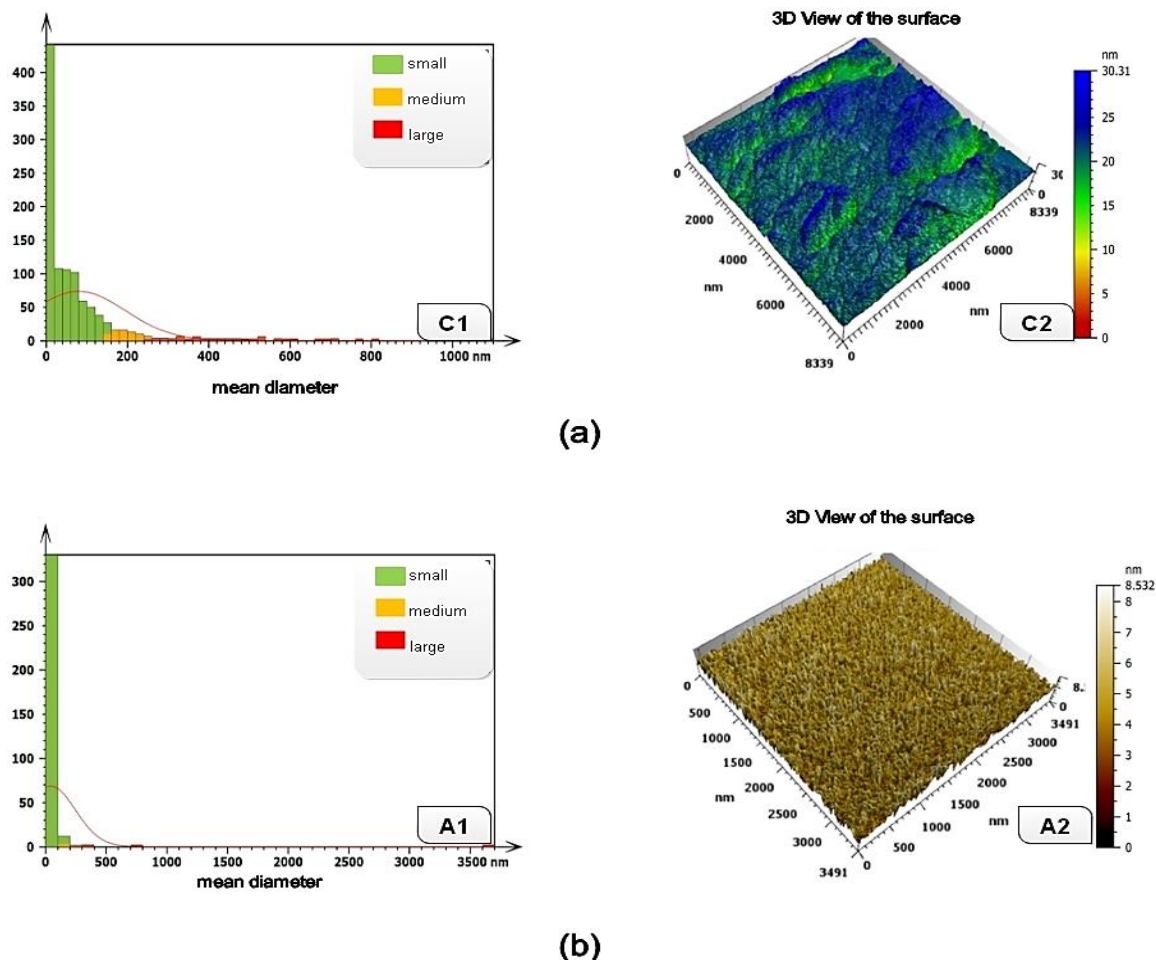


**Fig. 7.** Histogram for accumulated particles with the mean diameter and 3D view of the surface (1 refers to the histogram, and 2 refers to 3D AFM images), where (a) Cathode, (b) Anode

### 3.5. Congo red dye removal by EC-EO combined system

To detect the efficiency of prepared electrodes, they would be utilized as an anode for the EO process in an electrolytic cell besides Al as an anode for the EC process where the two processes are conducted simultaneously in one cell to eliminate Congo red dye.

400 mg of Congo red dye was dissolved in 2 L of distilled water, and to increase the conductivity of the electrolyte, 0.02M of  $\text{Na}_2\text{SO}_4$  was added in all experiments which did not affect the degradation of Congo red [25, 26]. Three parameter influences were studied; current density from 3 to 6  $\text{mA}/\text{cm}^2$ , (0 and 0.5)

$\text{g}/\text{l}$  of NaCl within (5, 10, 15, and 20) min as of electrolysis time. The results of Congo red removal efficiency were tabulated as shown in Table 3 and Table 4 with different parameters when the composite cathode or anode, respectively were used as anode for the EO process in a combined (EC-EO) system. The cathode showed higher efficiency than the anode for degradation of dye, due to its characterization and shape (large crystal size, more roughness, and granular shape) for the cathode which gave it a large surface area and more active sites compared with the anode and that agrees with the previous study [27].

**Table 3.** Congo red removal efficiency in the combined system (EC-EO) when using Al anode for the EC process and composite cathode as an anode for the EO process

Time (min.)	Current density (mA/cm <sup>2</sup> )	Congo red rem%, 0.5 (g/l) of NaCl	Congo red rem%, 0 (g/l) of NaCl	Current density (mA/cm <sup>2</sup> )	Congo red rem%, 0.5(g/l) of NaCl	Congo red rem%, 0 (g/l) of NaCl
5	6	46.04	44.31	3	37.3	40.84
10	6	92.10	88.63	3	75.26	85.68
15	6	95.25	94.11	3	87.89	92.84
20	6	98.00	96.57	3	95.20	96.00

**Table 4.** Congo red removal efficiency in the combined system (EC-EO) when using Al anode for the EC process and composite anode (A) as an anode for the EO process

Time (min.)	Current density (mA/cm <sup>2</sup> )	Congo red rem%, 0.5(g/l) of NaCl	Congo red rem%, 0 (g/l) of NaCl	Current density (mA/cm <sup>2</sup> )	Congo red rem%, 0.5(g/l) of NaCl	Congo red rem%, 0 (g/l) of NaCl
5	6	42.5	41.2	3	40.3	34.21
10	6	85	82.44	3	80.06	68.43
15	6	94.605	88.595	3	86.83	71.14
20	6	96.925	92.55	3	90.56	82.83

### 3.6. Effect of studies parameters

Hence the prepared composite cathode gave higher removal efficiency than the anode, it would be used as the main anode for the EO process in the following investigation.

#### 3.6.1. Effect of current density

The effect of current density on Congo red dye removal in an EC-EO combined system would be investigated in the presence and absence of NaCl within 20 min of electrolysis by utilizing Cu-Mn-Ni (prepared cathode) as anode for the EO process and Al as the anode for the EC process. The result showed in Fig. 8 a and Fig. 8 b, that as the current density increased from 3 to 6 mA/cm<sup>2</sup> the Congo red removal efficiency increased from 95.2% to 98%, respectively at 0.5g/l of NaCl. Also, it increased from 3 to 6 mA/cm<sup>2</sup> at 0 (g/l) of NaCl, removal efficiency increased from 96 % to 96.57%.

In the EC-EO combined process, the current density plays a crucial role in dye removal from both sides.,

During the electrocoagulation process, an increase in current density leads to an increase in Al<sup>+3</sup> ions that dissolve from the surface of the Aluminum electrode according to Faradys' law. This resulted in higher formation of Al (OH)<sub>3</sub> molecules that improve the removal of dyes and reduce energy and time consumption. This finding is consistent with previous studies. [28- 31]. Another reason for improving the coagulation process is the increase in the amount of oxygen (O<sub>2</sub>) produced on the anode surface besides hydrogen gas (H<sub>2</sub>) that formed at the cathode which in turn creates more small-sized bubbles that help increase the surface area for adsorption and more mass transfer attended, in addition to helping to float the collected dye molecule [32- 34]. Increasing C.D in the EO process caused more hydroxyl radical (OH<sup>•</sup>) generation that was generated in the direct electro-oxidation process and high formation of chlorine species (mainly HOCl at pH=7) as strong oxidized agents in NaCl medium, in previous studies similar results were observed [35- 37].

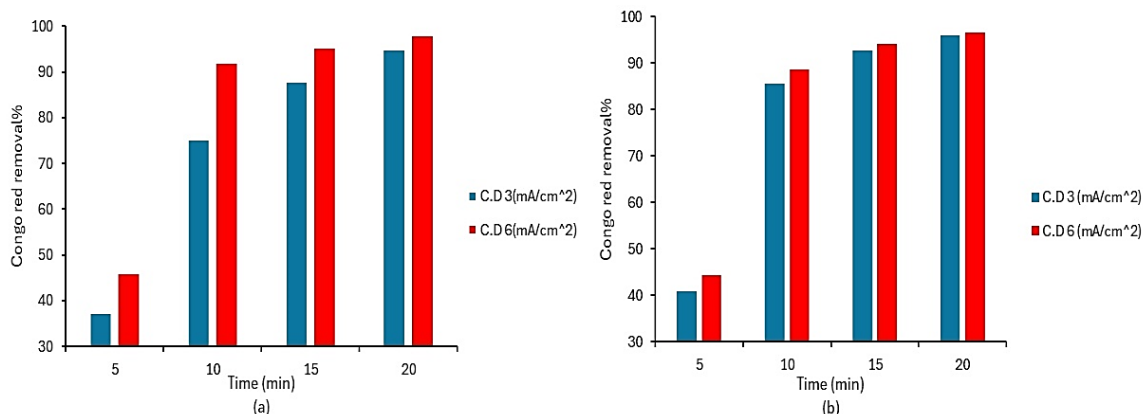


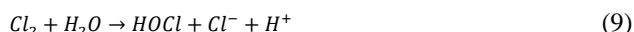
**Fig. 8.** Congo red removal efficiency in the combined system (EC-EO), Al anode for the EC process besides Cu-Mn-Ni as anode for the EO process, at Current Density (3-6) mA/cm<sup>2</sup>, Time= (5-10-15-20) min, and pH =7, (a) 0.5 g/l NaCl, (b) 0 (g/l) of NaCl

#### 3.6.2. Effect of NaCl concentration

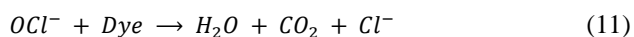
In Fig. 8 a and Fig. 8 b, the effect of NaCl addition was observed, after 20 min at pH=7 and 6 mA/cm<sup>2</sup> of applied

current density. In the EC-EO combined process, the Congo red removal efficiency enhanced from 96% to 98% when NaCl conc. increased from 0 to 0.5 g/l. These

results are attributed to several causes, increasing NaCl means an increase in conductivity of the electrolyte and current density easy to flow, resulting in more speed for electron transfer between the electrodes as a result of voltage and resistance decreasing. For the EO process, in direct electro-oxidation in the absence of NaCl hydroxyl radical (OH<sup>•</sup>) would be the only oxidizing agent in the system, while when NaCl is present in the system, more oxidizing agents would be generated like HOCl which is the main oxidizing agents at pH =7, as shown in Eqs. 8-10 [38], the same observation seen in the previous studies [39, 40].



HOCl and OCl<sup>-</sup> cause damage to the surface of dyes and organic particles and convert them to CO<sub>2</sub> and H<sub>2</sub>O.



Using the prepared electrode cathode of Cu-Mn-Ni as anode for the EO process showed different behavior from the prepared anode, in the presence of NaCl where the Congo red removal efficiency decreased as NaCl was added shown in Table 3 for example, at 0 g/l of NaCl, the Congo red removal efficiency was 85.68% at 3mA/cm<sup>2</sup>,10 min of electrolysis and its value was 75.26% at 3mA/cm<sup>2</sup>,10 min, and 0.5 g/l of NaCl. The reason for this could be explained as in an EC-EO combined system, excess of chlorine ions causes complex interaction with Al<sup>+3</sup> ions. This interaction reduces the positive charge precipitation on aluminum hydroxide, which affects the diffusion of metal ions and dye adsorption. Additionally, it can cause corrosion in the composite electrode (Cu-Mn-Ni), leading to the loss of a layer of coalesced oxides on

its surface and reduce in active sites, these findings are consistent with previous studies [32].

### 3.6.3. Effect of time

Time is a vital factor in the EC and EO process. The optimum removal efficiency was achieved after 20 min of electrolytic time, as seen in Fig. 8 a, the removal efficiency increased from 46.04% to 98% at 5 and 20 min, respectively at 6 mA/cm<sup>2</sup> and 0.5 g/l of NaCl conc., and when there was no salt added efficiency increased from 44.31% to 96.57% as shown in Fig. 8 b. These results can be explained by the fact that the efficiency of the EC process depends mainly on the electrode dissolution. According to Faraday's law, as time increases, more Al<sup>+3</sup> ions are released from the aluminum electrode, forming a large amount of aluminum hydroxide, and contributing to increased coagulated particles [41]. Regarding the electrochemical oxidation (EO) process, increasing the duration of the process can lead to a greater generation of hydroxyl radicals from the composite electrode, as well as an increase in hypochlorous acid in the salt medium. This can enhance the removal of dye and provide more time for the oxidized agent to come into contact with pollutant species [42, 43].

### 3.6.4. Comparison between EO and EC and combined (EC-EO) process

Few studies treated Congo red with a combined (EC-EO) system besides using ternary composite electrodes for the EO process [44, 45]. The outcomes of previous studies where EC and EO were employed separately to treat Congo red dye can be displayed in Table 5. It is evident that the combined process succeeded significantly in reducing the time and energy required for the removal process.

**Table 5.** Previous studies for congo red removal by EC and EO separated processes and combined EC-EO system in the present study

Process	Electrode type	Initial conc. (mg/l)	time (min)	Power supplied	Supporting electrolyte	pH	Congo red Removal %	Reference
EO	RuO <sub>2</sub> -IrO <sub>2</sub>	100	10	20 (mA/cm <sup>2</sup> )	2 (g/l) NaCl	7	98	[46]
EO	Pb/PbO <sub>2</sub>	20	20	10 (mA/cm <sup>2</sup> )	-		70	[47]
EO	BDD	500	540	30 (mA/cm <sup>2</sup> )	-	7	100	[48]
EO	Graphite	50	120	1.8 (mA/cm <sup>2</sup> )	5 (g/l) KCl	7.87	95	[49]
EC	Aluminum	65	29	8.75 (volt)	0	9.5	89.34	[50]
EC	Aluminum	100	30	14 (volt)	0.6 (g/l) NaCl	7	99	[51]
EC	Aluminum	100	60	200 (mA/cm <sup>2</sup> )	0	8	93	[52]
EC	Iron	60	15	40 (volt)	-	5	95	[53]
EC-EO	Al for EC, Composite Co-Mn-Ni for EO	200	20	6 (mA/cm <sup>2</sup> )	0.26 (g/l) NaCl	7	100	[45]
EC-EO	Al for EC, Cu-Mn-Ni (2:1:1) for EO	200	20	6 (mA/cm <sup>2</sup> )	0	7	99	[44]
EC-EO	Al for EC, Cu-Mn-Ni (1:1:1) for EO	200	20	6 (mA/cm <sup>2</sup> ), 3.2 (volt)	0.5 (g/l)NaCl	7	98	Present study
EC-EO	Al for EC, Cu-Mn-Ni for EO	200	20	6 (mA/cm <sup>2</sup> ), 3.9 (volt)	-	7	96.57	Present study



### 3.7. Energy consumption

To determine the energy required for removing Congo red dye from simulated water by using a combined system (EC-EO), by using the composite electrodes (C and A) as anode for the EO process besides Al as anode for the EC process, Table 6 would represent the energy consumption for the cathode (C) and Table 7 would represent the energy consumption for the anode (A), Eq. 12 was used to calculate energy consumption [54].

$$SCE = \frac{(V \cdot I \cdot t) \cdot 1000}{v \cdot (C_i - C_f)} \quad (12)$$

Where SCE is the energy consumption to remove the dye in kWh/kg of dye, V is the voltage applied (volte), I is current in (A), t is time for electrolysis in (h), v is the volume of treated solution in (l), C<sub>i</sub> and C<sub>f</sub> are the initial and final concentration of Congo red, respectively in mg/l. The result in Table 6 and Table 7 demonstrates that when the current density increases the value of energy consumption is increased as it is predictable. While, the increase of electrolyte conductivity and decrease in voltage when NaCl was added led to a decrease in SCE value.

**Table 6.** Effect of different parameters on energy consumption at pH =7 and Time =20 min, when a composite cathode (C) used as anode for the EO process in a combined (EC-EO) system

Time (min)	SCE (kWh/kg dye) for combined (EC-EO), Al as anode for the EC, and composite cathode as anode for the EO			
	C.D = 6 mA/cm <sup>2</sup>		C.D = 3 mA/cm <sup>2</sup>	
	NaCl conc.= 0.5 g/l	NaCl conc.= 0 g/l	NaCl conc.= 0.5 g/l	NaCl conc.= 0 g/l
5	0.960	1.096	0.403	0.450
10	0.882	1.178	0.318	0.342
15	1.284	1.644	0.512	0.593
20	1.666	2.086	0.625	0.758

**Table 7.** Effect of different parameters on energy consumption at pH =7 and Time =20 min, when a composite anode (A) used as anode for the EO process in a combined (EC-EO) system

Time (min)	SCE (kWh/kg dye) for combined (EC-EO), Al as anode for the EC, and composite Anode as anode for the EO			
	C.D = 6 mA/cm <sup>2</sup>		C.D = 3 mA/cm <sup>2</sup>	
	NaCl conc.=0.5 g/l	NaCl conc.=0 g/l	NaCl conc.= 0.5 g/l	NaCl conc.= 0 g/l
5	0.937	1.213	0.388	0.692
10	0.756	1.200	0.497	0.522
15	1.276	1.683	0.849	0.756
20	1.644	2.127	1.0749	0.857

## 4- Conclusion

Cu-Mn-Ni oxides were deposited on the surface of the graphite substrate by electrodeposition, 25mA/cm<sup>2</sup> was applied, and 0.075 M for each metal salt with a fixed mixing ratio 1:1:1 within 3h was utilized. The result of XRD, FE-SEM. EDX and AFM proved that several nano oxides such as CuO, Mn<sub>3</sub>O<sub>4</sub>, and NiO were deposited on the cathode and anode surface, a smooth surface was obtained on the cathode and anode, and crystalline

occurred on the cathode more than anode. The prepared electrodes (cathode and anode) were used as anode for the EO process besides Al for the EC process in the combined system, to remove Congo red dye. The effect of current density, NaCl conc., and time was studied for the combined removal process.

Experimental results revealed that the composite cathode is more efficient than the composite anode due to its larger crystal size, and rougher, in addition to the granular shape of its surface. Composite electrodes have high efficiency in the direct and indirect electro-oxidation processes, maximum efficiency was obtained at 91% at 6mA/cm<sup>2</sup> with 1.6655381 (kWh/kg dye) as energy consumption when 0.5 g/l of NaCl salt was added within 20 min of electrolysis time, the comparison of the present result with the results in the previous studies when the EC and EO used separately to eliminate Congo red, it was concluded that combine process (EC-EO) when the two processes operate at the same electrolytic cell with using a composite electrode as anode for EO process improved the removal efficiency and led to decreased the time and consumed energy.

## Nomenclature

Nomenclature	Meaning
Unit	
C.D	Current density
mA/cm <sup>2</sup>	
C <sub>i</sub>	Initial Congo red concentration
mg/l	
C <sub>f</sub>	Final Congo red concentration
mg/l	
SCE	Energy consumption
kWh/kg of dye	
Symbol	Definition
AFM	Atomic force microscopy
EDX	Energy-dispersive X-ray
spectrometry	
FE-SEM	Field emission scanning
electronic microscopy	
HOCl	Hypochlorous acid
OH <sup>•</sup>	Hydroxyl radical
OCl <sup>-</sup>	Hypochlorite ion
XRD	X-ray diffraction

## Reference

- [1] C. FN and M. MF, "Factors Affecting Water Pollution: A Review," *Journal of Ecosystem & Ecography*, vol. 07, no. 01, pp. 6–8, 2017, <https://doi.org/10.4172/2157-7625.1000225>
- [2] D. Jacquemin, E. A. Perpète, I. Ciofini, and C. Adamo, "Accurate Simulation of Optical Properties in Dyes," *Accounts of Chemical Research*, vol. 42, no. 2, pp. 326–334, Feb. 2009, <https://doi.org/10.1021/ar800163d>

- [3] Z. Carmen and S. Daniela, *Textile organic dyes-characteristics, polluting effects and separation/elimination procedures from industrial effluents-a critical overview*, vol. 3. IntechOpen Rijeka, 2012.
- [4] A. Akhtar, Z. Aslam, A. Asghar, M. M. Bello, and A. A. Raman, "Electrocoagulation of Congo Red dye-containing wastewater: Optimization of operational parameters and process mechanism," *Journal of Environmental Chemical Engineering*, vol. 8, no. 5, p. 104055, Oct. 2020, <https://doi.org/10.1016/j.jece.2020.104055>
- [5] R. R. M. Khan et al., "Biological and Photocatalytic Degradation of Congo Red, a Diazo Sulfonated Substituted Dye: a Review," *Water, Air, Soil Pollution*, vol. 233, no. 11, p. 468, Nov. 2022, <https://doi.org/10.1007/s11270-022-05935-9>
- [6] R. Saleh and A. Taufik, "Degradation of methylene blue and congo-red dyes using Fenton, photo-Fenton, sono-Fenton, and sonophoto-Fenton methods in the presence of iron(II,III) oxide/zinc oxide/graphene (Fe<sub>3</sub>O<sub>4</sub>/ZnO/graphene) composites," *Separation and Purification Technology*, vol. 210, pp. 563–573, Feb. 2019, <https://doi.org/10.1016/j.seppur.2018.08.030>
- [7] M. Faouzi Elahmadi, N. Bensalah, and A. Gadri, "Treatment of aqueous wastes contaminated with Congo Red dye by electrochemical oxidation and ozonation processes," *Journal of Hazardous Materials*, vol. 168, no. 2–3, pp. 1163–1169, 2009, <https://doi.org/10.1016/j.jhazmat.2009.02.139>
- [8] F. C. Moreira, R. A. R. Boaventura, E. Brillas, and V. J. P. Vilar, "Electrochemical advanced oxidation processes: A review on their application to synthetic and real wastewaters," *Applied Catalysis B: Environmental*, vol. 202, pp. 217–261, Mar. 2017, <https://doi.org/10.1016/j.apcatb.2016.08.037>
- [9] S. A. Abdul-Husain and S. Alramahi, "Removal of Pathogenic pollutants using electrocoagulation using aluminium electrodes," *IOP Conference Series: Materials Science and Engineering*, vol. 1184, no. 1, p. 012011, Sep. 2021, <https://doi.org/10.1088/1757-899X/1184/1/012011>
- [10] R. H. Salman, E. M. Khudhair, K. M. Abed, and A. S. Abbas, "Removal of E133 brilliant blue dye from artificial wastewater by electrocoagulation using cans waste as electrodes," *Environmental Progress Sustainable Energy*, vol. 43, no. 2, Mar. 2024, <https://doi.org/10.1002/ep.14292>
- [11] C. A. Damalas and I. G. Eleftherohorinos, "Pesticide Exposure, Safety Issues, and Risk Assessment Indicators," *International Journal of Environmental Research and Public Health*, vol. 8, no. 5, pp. 1402–1419, May 2011, <https://doi.org/10.3390/ijerph8051402>
- [12] P. Y. Lim et al., "Improved stability of titanium based boron-doped chemical vapor deposited diamond thin-film electrode by modifying titanium substrate surface," *Thin Solid Films*, vol. 516, no. 18, pp. 6125–6132, Jul. 2008, <https://doi.org/10.1016/j.tsf.2007.11.016>
- [13] X. Cui, G. Zhao, Y. Lei, H. Li, P. Li, and M. Liu, "Novel vertically aligned TiO<sub>2</sub> nanotubes embedded with Sb-doped SnO<sub>2</sub> electrode with high oxygen evolution potential and long service time," *Materials Chemistry and Physics*, vol. 113, no. 1, pp. 314–321, Jan. 2009, <https://doi.org/10.1016/j.matchemphys.2008.07.087>
- [14] H. J. Nsaif, N. S. Majeed, R. H. Salman, and K. M. Abed, "Elimination of phenol by sonoelectrochemical process utilizing graphite, stainless steel, and titanium anodes: optimization by taguchi approach", *Iraqi Journal of Chemical and Petroleum Engineering*, vol. 25, no. 3, pp. 21–30, Sep. 2024, <https://doi.org/10.31699/IJCPE.2024.3.3>
- [15] E. M. Abebe and M. Ujihara, "Simultaneous Electrodeposition of Ternary Metal Oxide Nanocomposites for High-Efficiency Supercapacitor Applications," *ACS Omega*, 2022, <https://doi.org/10.1021/acsomega.2c00826>
- [16] C. Clavijo and J. F. Osma, "Functionalized leather: A novel and effective hazardous solid waste adsorbent for the removal of the diazo dye congo red from aqueous solution," *Water (Switzerland)*, vol. 11, no. 9, 2019, <https://doi.org/10.3390/w11091906>
- [17] H. Q. Ali and A. A. Mohammed, "Elimination of Congo Red Dyes From Aqueous Solution Using Eichhornia Crassipes," *Iraqi Journal of Chemical and Petroleum Engineering*, vol. 21, no. 4, pp. 21–32, 2020. <https://doi.org/10.31699/ijcpe.2020.4.3>
- [18] H. H. Thwaini and R. H. Salman, "Modification of Electro-Fenton Process with Granular Activated Carbon for Phenol Degradation – Optimization by Response Surface Methodology," *Journal of Ecological Engineering*, vol. 24, no. 9, pp. 92–104, Sep. 2023, <https://doi.org/10.12911/22998993/168411>
- [19] Y. A. Ahmed and R. H. Salman, "Simultaneous electrodeposition of multicomponent of Mn–Co–Ni oxides electrodes for phenol removal by anodic oxidation," *Case Studies in Chemical and Environmental Engineering*, p. 100386, 2023. <https://doi.org/10.1016/j.csee.2023.100386>
- [20] S. E. S. Monica, C. R. Dhas, R. Venkatesh, R. Sivakumar, R. Vignesh, and V. A. Ferby, "Nebulizer sprayed nickel-manganese (Ni-Mn) mixed metal oxide nanocomposite coatings for high-performance electrochromic device applications," *Journal of Solid State Electrochemistry*, vol. 26, no. 5, pp. 1271–1290, 2022. <https://doi.org/10.1007/s10008-022-05159-1>
- [21] P. Zhang et al., "Dendritic core-shell nickel-iron-copper metal/metal oxide electrode for efficient electrocatalytic water oxidation," *Nature Communications*, vol. 9, no. 1, p. 381, Jan. 2018, <https://doi.org/10.1038/s41467-017-02429-9>

- [22] Z. I. Abbas and A. S. Abbas, "Oxidative degradation of phenolic wastewater by electro-fenton process using MnO<sub>2</sub>-graphite electrode," *Journal of Environmental Chemical Engineering*, vol. 7, no. 3, p. 103108, 2019, <https://doi.org/10.1016/j.jece.2019.103108>
- [23] N. F. El Boraei and M. A. M. Ibrahim, "Black binary nickel cobalt oxide nano-powder prepared by cathodic electrodeposition; characterization and its efficient application on removing the Remazol Red textile dye from aqueous solution," *Materials Chemistry and Physics*, vol. 238, no. June, p. 121894, 2019, <https://doi.org/10.1016/j.matchemphys.2019.121894>
- [24] N. L. Torad et al., "Direct Synthesis of MOF-Derived Nanoporous Carbon with Magnetic Co Nanoparticles toward Efficient Water Treatment," *Small*, vol. 10, no. 10, pp. 2096–2107, May 2014, <https://doi.org/10.1002/sml.201302910>
- [25] R. M. Belal, M. A. Zayed, R. M. El-Sherif, and N. A. A. Ghany, "Advanced electrochemical degradation of basic yellow 28 textile dye using IrO<sub>2</sub>/Ti meshed electrode in different supporting electrolytes," *Journal of Electroanalytical Chemistry*, vol. 882, p. 114979, 2021, <https://doi.org/10.1016/j.jelechem.2021.114979>
- [26] Z. Zhang and P. Wang, "Highly stable copper oxide composite as an effective photocathode for water splitting via a facile electrochemical synthesis strategy," *Journal of Material Chemical*, vol. 22, no. 6, pp. 2456–2464, 2012, <https://doi.org/10.1039/C1JM14478B>
- [27] Y. A. Ahmed, R. H. Salman, and F. Kandemirli, "Anodic and Cathodic preparation of MnO<sub>2</sub>/Co<sub>2</sub>O<sub>3</sub> Composite Electrode Anodes for Electro-Oxidation of Phenol," *Iraqi Journal of Chemical and Petroleum Engineering*, vol. 24, no. 4, pp. 115–125, 2023, <https://doi.org/10.31699/IJCPE.2023.4.12>
- [28] B. A. Abdulhadi, P. Kot, K. S. Hashim, A. Shaw, and R. Al Khaddar, "Influence of current density and electrodes spacing on reactive red 120 dye removal from dyed water using electrocoagulation/electroflotation (EC/EF) process," *IOP Conference Series: Materials Science and Engineering*, vol. 584, no. 1, p. 012035, Aug. 2019, <https://doi.org/10.1088/1757-899X/584/1/012035>
- [29] A. Othmani, A. Kesraoui, and M. Seffen, "The alternating and direct current effect on the elimination of cationic and anionic dye from aqueous solutions by electrocoagulation and coagulation flocculation," *Euro-Mediterranean Journal for Environmental Integration*, vol. 2, no. 1, p. 6, Oct. 2017, <https://doi.org/10.1007/s41207-017-0016-y>
- [30] S. C. M. Signorelli, J. M. Costa, and A. F. de Almeida Neto, "Electrocoagulation-flotation for orange II dye removal: Kinetics, costs, and process variables effects," *Journal of Environmental Chemical Engineering*, vol. 9, no. 5, p. 106157, Oct. 2021, <https://doi.org/10.1016/j.jece.2021.106157>
- [31] B. K. Nandi and S. Patel, "Effects of operational parameters on the removal of brilliant green dye from aqueous solutions by electrocoagulation," *Arabian Journal of Chemistry*, vol. 10, pp. S2961–S2968, May 2017, <https://doi.org/10.1016/j.arabjc.2013.11.032>
- [32] R. H. Salman and A. H. Abbar, "Optimization of a combined electrocoagulation-electro-oxidation process for the treatment of Al-Basra Majnoon Oil field wastewater: Adopting a new strategy," *Chemical Engineering and Processing - Process Intensification*, vol. 183, p. 109227, 2023, <https://doi.org/10.1016/j.cep.2022.109227>
- [33] A. A. Beddai, B. A. Badday, A. M. Al-Yaqoobi, M. K. Mejbel, Z. S. Al Hachim, and M. K. A. Mohammed, "Color Removal of Textile Wastewater Using Electrochemical Batch Recirculation Tubular Upflow Cell," *International Journal of Chemical Engineering*, vol. 2022, pp. 1–8, Mar. 2022, <https://doi.org/10.1155/2022/4713399>
- [34] M. Elazzouzi, K. Haboubi, and M. S. Elyoubi, "Enhancement of electrocoagulation-flotation process for urban wastewater treatment using Al and Fe electrodes: techno-economic study," *Material Today Proceedings*, vol. 13, pp. 549–555, 2019, <https://doi.org/10.1016/j.matpr.2019.04.012>
- [35] S. El Aggadi, Z. El Abbassi, and A. El Hourch, "Color removal from dye-containing aqueous solutions by electrooxidation," *Desalination and Water Treatment*, vol. 215, pp. 232–236, 2021, <https://doi.org/10.5004/dwt.2021.26766>
- [36] F. Agustina, A. Y. Bagastyo, and E. Nurhayati, "Electro-oxidation of landfill leachate using boron-doped diamond: role of current density, pH and ions," *Water Science and Technology*, vol. 79, no. 5, pp. 921–928, Mar. 2019, <https://doi.org/10.2166/wst.2019.040>
- [37] F. E. Titchou et al., "Electrochemical oxidation treatment of Direct Red 23 aqueous solutions: Influence of the operating conditions," *Separation Science and Technology*, vol. 57, no. 9, pp. 1501–1520, Jun. 2022, <https://doi.org/10.1080/01496395.2021.1982978>
- [38] B. Cifcioglu-Gozuacik et al., "Efficient removal of ammoniacal nitrogen from textile printing wastewater by electro-oxidation considering the effects of NaCl and NaOCl addition," *Water Science and Technology*, vol. 84, no. 3, pp. 752–762, Aug. 2021, <https://doi.org/10.2166/wst.2021.261>
- [39] S. Singh, S. L. Lo, V. C. Srivastava, and A. D. Hiwarkar, "Comparative study of electrochemical oxidation for dye degradation: Parametric optimization and mechanism identification," *Journal of Environmental Chemical Engineering*, vol. 4, no. 3, pp. 2911–2921, Sep. 2016, <https://doi.org/10.1016/j.jece.2016.05.036>

- [40] A. Abdelhay, I. Jum'h, A. Albsoul, D. Abu Arideh, and B. Qatanani, "Performance of electrochemical oxidation over BDD anode for the treatment of different industrial dye-containing wastewater effluents," *Water Reuse*, vol. 11, no. 1, pp. 110–121, Mar. 2021, <https://doi.org/10.2166/wrd.2020.064>
- [41] N. Liu and Y. Wu, "Removal of methylene blue by electrocoagulation: a study of the effect of operational parameters and mechanism," *International Journal of Ionics – The Science and Technology of Ionic Motion*, vol. 25, no. 8, pp. 3953–3960, Aug. 2019, <https://doi.org/10.1007/s11581-019-02915-8>
- [42] H. N. Ibarra-Taquez, E. GilPavas, E. R. Blatchley, M.-Á. Gómez-García, and I. Dobrosz-Gómez, "Integrated electrocoagulation-electrooxidation process for the treatment of soluble coffee effluent: Optimization of COD degradation and operation time analysis," *Journal of Environmental Management*, vol. 200, pp. 530–538, Sep. 2017, <https://doi.org/10.1016/j.jenvman.2017.05.095>
- [43] I. Dobrosz-Gómez and M. Á. Gómez-García, "Treatment of soluble coffee industrial effluent by electro-coagulation–electro-oxidation process: multiobjective optimization and kinetic study," *International Journal of Environmental Science and Technology* vol. 19, no. 7, pp. 6071–6088, Jul. 2022, <https://doi.org/10.1007/s13762-021-03562-1>
- [44] R. A. Jasim and R. H. Salman, "Congo red removal from aqueous solution by electrocoagulation- electro-oxidation combined system with Al and Cu–Mn–Ni nano composite as efficient electrodes," *Case Studies in Chemical and Environmental Engineering*, vol. 9, p. 100747, Jun. 2024, <https://doi.org/10.1016/j.cscee.2024.100747>
- [45] R. A. Jasim and R. H. Salman, "Use of Nano Co-Ni-Mn Composite and Aluminum for Removal of Artificial Anionic Dye Congo Red by Combined System," *Ecological Engineering & Environmental Technology*, vol. 25, no. 7, pp. 133–149, Jul. 2024, <https://doi.org/10.12912/27197050/188266>
- [46] K. Sathishkumar, M. S. AlSalhi, E. Sanganyado, S. Devanesan, A. Arulprakash, and A. Rajasekar, "Sequential electrochemical oxidation and biotreatment of the azo dye congo red and textile effluent," *Journal of Photochemistry and Photobiology B: Biology*, vol. 200, p. 111655, 2019, <https://doi.org/10.1016/j.jphotobiol.2019.111655>
- [47] Z. Chen et al., "A novel Pb/PbO<sub>2</sub> electrodes prepared by the method of thermal oxidation-electrochemical oxidation: Characteristic and electrocatalytic oxidation performance," *Journal of Alloys and Compounds*, vol. 851, p. 156834, Jan. 2021, <https://doi.org/10.1016/j.jallcom.2020.156834>
- [48] M. Faouzi Elahmadi, N. Bensalah, and A. Gadri, "Treatment of aqueous wastes contaminated with Congo Red dye by electrochemical oxidation and ozonation processes," *Journal of Hazardous Materials*, vol. 168, no. 2–3, pp. 1163–1169, 2009, <https://doi.org/10.1016/j.jhazmat.2009.02.139>
- [49] R. Kaur and H. Kaur, "Electrochemical degradation of Congo red from aqueous solution: role of graphite anode as electrode material," *Portugaliae Electrochimica Acta*, vol. 34, no. 3, pp. 185–196, 2016, <https://doi.org/10.4152/pea.201603185>
- [50] M. S. Ramya Sankar and V. Sivasubramanian, "Application of statistical design to optimize the electrocoagulation of synthetic Congo red dye solution and predicting the mechanism," *International Journal of Environmental Science and Technology*, vol. 17, no. 3, pp. 1373–1386, Mar. 2020, <https://doi.org/10.1007/s13762-019-02555-5>
- [51] Z. A. Sadoon and M. J. M-Ridha, "Removal of Reactive Dyes by Electro Coagulation Process from Aqueous Solution," *Journal of Engineering*, vol. 26, no. 2, pp. 14–28, Jan. 2020, <https://doi.org/10.31026/j.eng.2020.02.02>
- [52] M. S. R. Sankar et al., "Kinetic, isothermal and thermodynamic investigation on electrocoagulation of Congo Red dye removal from synthetic wastewater using aluminium electrodes," *Desalination and Water Treatment*, vol. 122, pp. 339–350, 2018, <https://doi.org/10.5004/dwt.2018.23082>
- [53] A. Suresh, S. Sathish, and G. Narendrakumar, "Electrocoagulation of azo dye containing synthetic wastewater using monopolar iron electrodes and the characterization of the sludge," *Water Practice & Technology*, vol. 14, no. 3, pp. 587–597, Sep. 2019, <https://doi.org/10.2166/wpt.2019.044>
- [54] F. Ilhan, K. Ulucan-Altuntas, Y. Avsar, U. Kurt, and A. Saral, "Electrocoagulation process for the treatment of metal-plating wastewater: Kinetic modeling and energy consumption," *Frontiers of Environmental Science & Engineering*, vol. 13, no. 5, p. 73, Oct. 2019, <https://doi.org/10.1007/s11783-019-1152-1>

## ازالة الصبغة الايونية بواسطة التخثر الكهربائي والأكسدة الكهربائية المدمجتين باستخدام قطب الالمنيوم و أقطاب (Cu-Mn-Ni) النانوية المصنعة

ريمان عبود جاسم<sup>١\*</sup>، رشا حبيب سلمان<sup>١</sup>، مهند زيار<sup>٢</sup>

<sup>١</sup> قسم الهندسة الكيميائية، كلية الهندسة، جامعة بغداد، بغداد، العراق

<sup>٢</sup> قسم الهندسة الكيميائية، جامعة كيرتن، استراليا

### الخلاصة

تعد الطريقة المدمجة (التخثر الكهربائي والأكسدة الكهربائية) من الطرق الواعدة في عملية ازالة الملوثات من الماء، في هذا العمل تم دمج العمليتين معا في نفس الخلية حيث تم ازالة ٢٠٠ ملغم/لتر من صبغة الكونغو الاحمر باستخدام ثلاثة اقطاب من الستنلس ستيل ككاثود للعملياتين وقطب الالمنيوم كأنود لعملية التخثر الكهربائي وتم تصنيع قطب ثالث عن طريق ترسب مجموعة من اكاسيد النحاس والمنغنيز والنيكل على سطح الكرافيت باستخدام الترسيب الكهربائي حيث تم اذابة ٠,٠٧٥ مولاري من نترات النحاس والنيكل وكلوريد المنغنيز في الماء المقطر وبنسب وزنية ثابتة ١:١:١ حيث تم الترسيب في ان واحد على سطح الكاثود والانود باستخدام تيار ثابت ٢٥ ملي امبير/سم<sup>٢</sup> لمدة ثلاث ساعات (ساعة ونصف لكل جهة من الاقطاب) بدرجة حرارة الغرفة، ثم تمت كلستها باستخدام الاقران وبدرجة حرارة ٤٠٠ درجة سيليزية لمدة ساعة واحدة. تم تحديد البنية النانوية وشكل الأكاسيد النانوية المتجمعة على سطح المعدن باستخدام جهاز حيود الاشعة السينية والمجهر الالكتروني والاشعة السينية المشتتة ومجهر القوة الذرية. أثبتت الفحوصات ترسب الاكاسيد النانوية الثلاثة على سطح الكاثود والانود. كانت الاقطاب المصنعة كفاءة جدا عند استخدامها كأنود في عملية الأكسدة الكهربية كما ان العملية المدمجة (التخثر الكهربائي والأكسدة الكهربائية) لها قابلية على ازالة مايزيد عن ٩٨% و ٥٧.٩٦% من صبغة الكونغو الحمراء بوجود وعدم وجود ملح كلوريد الصوديوم على التوالي عن طريق استخدام ٦ ملي امبير/سم<sup>٢</sup> ولمدة ٢٠ دقيقة.

الكلمات الدالة: الترسيب الكهربائي، الاقطاب المصنعة، التخثر الكهربائي، الأكسدة الكهربائية، النظام المدمج، صبغة الكونغو الأحمر.